





A fresh look at the nuclear transparency using the generalized parton distributions (GPDs)

The MMGPDs Collaboration:

Muhammad Goharipour ^{1,2,*} Fatemeh Irani ^{3,†} K. Azizi ^{3,4,2,‡}

And

Dipankar Dutta ^{5,§}

¹*School of Physics, Institute for Research in Fundamental Sciences (IPM), P.O. Box 19395-5531, Tehran, Iran*

²*School of Particles and Accelerators, Institute for Research in Fundamental Sciences (IPM), P.O. Box 19395-5746, Tehran, Iran*

³*Department of Physics, University of Tehran, North Karegar Avenue, Tehran 14395-547, Iran*

⁴*Department of Physics, Dogus University, Dudullu-Ümraniye, 34775 İstanbul, Türkiye*

⁵*Mississippi State University, Mississippi State, MS 39762, USA*

Color transparency (CT) is a fundamental phenomenon in quantum chromodynamics (QCD) where hadrons produced in high-energy exclusive processes traverse nuclear matter with minimal interactions. Nuclear transparency, which quantifies this attenuation suppression, is a quantity with high sensitivity to CT effects and provides critical insights into QCD dynamics in nuclear environments. In this study, we revisit nuclear transparency using the framework of generalized parton distributions (GPDs). By constructing nuclear GPDs (nGPDs) through the incorporation of nuclear parton distribution functions (nPDFs), we calculate the nuclear transparency $T(Q^2)$ for the carbon nucleus as a function of momentum transfer Q^2 considering various definitions and compare the results obtained with available experimental data. Our finding highlights the importance of choosing a physically motivated definition of nuclear transparency. Moreover, we emphasize that a more reliable determination of nGPDs requires a dedicated global analysis incorporating nuclear data. Such an approach is essential for improving the theoretical understanding of CT and for achieving consistency with experimental observations in the high- Q^2 regime.

Introduction Color transparency (CT) is an important phenomenon in quantum chromodynamics (QCD) wherein hadrons produced in high-energy (exclusive) processes traverse nuclear matter with minimal interaction [1]. This behavior occurs when the hadron forms a compact, color-neutral configuration, effectively rendering it “invisible” to the surrounding nuclear medium due to the cancellation of its color fields. As a result, we see a significant suppression in the usual strong interaction between the hadron and the nucleons. This property becomes particularly important in high-momentum-transfer reactions, where small-size color singlet states are favored. The concept is closely tied to nuclear transparency, which quantifies how easily particles can propagate through a nucleus [2]. High nuclear transparency indicates reduced attenuation of the particle as it moves through nuclear matter. So, it can provide a sensitive test for the presence of CT effects. Studies have shown that lighter nuclei typically exhibit higher transparency, and as the energy of the interaction increases, the nucleus is expected to be more transparent. Ongoing and future experiments continue to explore how nuclear transparency varies across energy scales and target materials [2–5]. Precise measurements of nuclear transparency, particularly at higher values of momentum transfer (Q^2), provide critical insight into the dynamics of QCD in nuclear environments. Consequently, color transparency and nuclear transparency have always been important subjects to investigate in recent years (see, e.g, Refs. [6–12]).

Generalized parton distributions (GPDs) provide a unified

description of the longitudinal-momentum and transverse-position correlations of quarks and gluons inside hadrons. Therefore, they enable us to study the hadron structure, particularly the nucleons, in three dimensions [13–17]. They are experimentally accessed through hard exclusive processes such as deeply virtual Compton scattering (DVCS) and deeply virtual meson production (DVMP) whose factorization properties allow a clean extraction of GPDs over a wide kinematic range [18–24]. GPDs are also related to familiar hadronic observables, connecting directly to electromagnetic, axial, gravitational, and transition form factors (FFs) [25–31]. It should be noted that GPDs are reduced to ordinary parton distribution functions (PDFs) at the so-called forward limit. When the process involves a nucleus rather than a free proton, medium effects encoded in nuclear PDFs (nPDFs) for the inclusive processes or nuclear GPDs (nGPDs) for the elastic and hard exclusive processes must be taken into account.

It was shown that the nuclear transparency can be calculated using GPDs [32, 33]. Hence, the precise measurements of nuclear transparency can put new constraints on GPDs and their nuclear modifications. According to QCD predictions, nuclear transparency should exhibit a characteristic rise with increasing Q^2 due to the CT phenomenon. However, recent high-precision measurements of the nuclear transparency of protons [34] challenge this expectation. Actually, the measured nuclear transparency of carbon has been found to be both energy and Q^2 independent up to $Q^2 = 14.2 (\text{GeV}/c)^2$. In the present study, we revisit the nuclear transparency phenomenon through the lens of GPDs, aiming to reconcile these experimental findings with theoretical expectations. Our investigation provides new insights into the interplay between GPDs and CT in the high- Q^2 regime.

Nuclear Transparency The phenomenon of color transparency is a specific prediction of QCD [1] which states that

* muhammad.goharipour@ipm.ir; Corresponding author

† f.irani@ut.ac.ir

‡ kazem.azizi@ut.ac.ir

§ d.dutta@msstate.edu

hadrons (like protons or pions) produced in high-momentum-transfer reactions may interact weakly with the nuclear medium while transiting through it. Based on this concept, many experimental efforts have been performed to measure the nuclear transparency [34–42] which refers to the degree to which a nucleus allows particles to pass through it. Such measurements help describe how “transparent” a nucleus appears to incoming particles, particularly in high-energy collisions. If the nucleus is highly transparent, the particles exit with little energy loss or deflection. It is well established now that transparency is influenced by nuclear density; light nuclei (like carbon) are more transparent than heavy ones (like gold) [1]. Also, at very high energies (e.g., in deep inelastic scattering), the nucleus becomes completely transparent.

From an experimental point of view, nuclear transparency can be measured by studying how particles (such as protons, pions, or electrons) interact with nuclei in high-energy collisions. One of the reactions used to measure nuclear transparency is the quasielastic scattering where a high-energy electron (e) is fired at a nucleus with mass number A such as those performed at Jefferson Lab (JLab) and SLAC [34]. Due to the scattering, a nucleus with mass number $A - 1$ is produced in the final state by knocking out a proton (p) from the parent nucleus, $e + A \rightarrow e' + p + (A - 1)$. The nuclear transparency can be measured by detecting the scattered electron (e') and ejected proton. To be more precise, the nuclear transparency $T(Q^2)$, where Q is the 4-momentum transfer, is defined as the ratio of experimental yield ($Y_{\text{exp}}(E_m, \vec{p}_m)$) to the expected theoretical yield for a non-interacting proton ($Y_{\text{theo}}(E_m, \vec{p}_m)$) [34], such as those calculated assuming the plane-wave impulse approximation (PWIA) [43]:

$$T(Q^2) = \frac{\int_V d^3p_m dE_m Y_{\text{exp}}(E_m, \vec{p}_m)}{\int_V d^3p_m dE_m Y_{\text{theo}}(E_m, \vec{p}_m)}. \quad (1)$$

Note that Y_{exp} and Y_{theo} are integrated over the same phase space volume V . Here, $E_m = \nu - T_{p'} - T_{A-1}$ and $\vec{p}_m = \vec{p}_{p'} - \vec{q}$ are the missing energy and momentum, respectively, where $T_{p'}$ and $\vec{p}_{p'}$ represents the kinetic energy and momentum of knocked out protons, and T_{A-1} is the reconstructed kinetic energy of the $A - 1$ recoiling nucleus. As usual, ν and \vec{q} are the energy and momentum transfer, respectively, which can be determined using the electron beam energy or momentum of the incoming electron (E_e/\vec{p}_e) and the scattered electron ($E_{e'}/\vec{p}_{e'}$) as $\nu = E_e - E_{e'}$ and $\vec{q} = \vec{p}_e - \vec{p}_{e'}$.

As a result, if $T \approx 1$, the nucleus is nearly transparent while if $T \ll 1$, the proton is strongly absorbed. Note that the nuclear transparency can also be measured through the hadronic collisions [44–50] such as those performed at the LHC. By comparing yields from light (e.g., carbon) versus heavy (e.g., lead) nuclei, one can measure the transparency. If protons exit with minimal energy loss, the nucleus is more transparent.

GPDs at zero skewness It is well established now that GPDs can provide a powerful framework for probing the three-dimensional (3D) structure of hadrons, especially nucleons [13–17]. They can be accessed through hard exclusive processes such as DVCS and DVMP [18–24]. In contrary to the ordinary PDFs, which depend only on the longitudinal momentum fraction x and the factorization scale μ , GPDs depend

also to the negative momentum transverse squared, $t = -Q^2$, and the longitudinal momentum transverse (skewness parameter), ξ . GPDs at zero skewness are also an essential ingredient of different types of elastic scattering processes because they are related to different types of hadron FFs including the electromagnetic, axial, gravitational, and transition FFs [25–31].

The unpolarized valence GPDs $H_v^q(x, t)$ and $E_v^q(x, t)$ at zero skewness ($\xi = 0$) for quark flavors $q = u, d$ (neglecting the strange-quark contribution) can be determined through a global analysis of the experimental data of the electromagnetic FFs and elastic electron-proton cross sections, as demonstrated by the MMGPDs Collaboration [30, 51]. This approach utilizes two fundamental relations: First, the connection between nucleon FFs and GPDs which is established through the following sum rules [27, 52]:

$$\begin{aligned} F_1(Q^2) &= \sum_q e_q F_1^q(Q^2) = \sum_q e_q \int_0^1 dx H_v^q(x, \mu^2, Q^2), \\ F_2(Q^2) &= \sum_q e_q F_2^q(Q^2) = \sum_q e_q \int_0^1 dx E_v^q(x, \mu^2, Q^2), \end{aligned} \quad (2)$$

where F_1 and F_2 are the Dirac and Pauli form factors, respectively, and e_q refers to the electric charge of the constituent quark q . Note that the neutron (n) FFs can be obtained by considering the isospin symmetry $u^p = d^n$, $d^p = u^n$. Second, the relation between these FFs and the Sachs electromagnetic FFs:

$$\begin{aligned} G_M(Q^2) &= F_1(Q^2) + F_2(Q^2), \\ G_E(Q^2) &= F_1(Q^2) - \frac{Q^2}{4m^2} F_2(Q^2). \end{aligned} \quad (3)$$

By employing these relations within a χ^2 minimization framework, and adopting suitable parameterizations for H and E , one can extract the GPDs from experimental data on $G_E(Q^2)$, $G_M(Q^2)$, and differential cross sections (or reduced cross sections).

Building on the MMGPDs Collaboration’s framework [30, 51], the valence quark GPDs are parameterized through the following ansatz:

$$\begin{aligned} H_v^q(x, \mu^2, t) &= q_v(x, \mu^2) \exp[t f_v^q(x)], \\ E_v^q(x, \mu^2, t) &= e_v^q(x, \mu^2) \exp[t g_v^q(x)], \end{aligned} \quad (4)$$

where $q_v(x, \mu^2)$ represents the unpolarized valence quark PDF and the profile functions $f_v^q(x)$ and $g_v^q(x)$ follow the general form:

$$\mathcal{F}(x) = \alpha'(1-x)^3 \log \frac{1}{x} + B(1-x)^3 + Ax(1-x)^2. \quad (5)$$

This parameterization successfully describes the experimental data while naturally reducing to standard PDFs in the forward limit ($t = 0$, $\xi = 0$).

For GPD H , the MMGPDs Collaboration employed next-to-leading order (NLO) NNPDF valence quark distributions [53] at $\mu = 2$ GeV as the forward limit. However, since

no experimental parametrization exists for the forward limit $e_v^q(x)$ of GPD E , the collaboration determined it through a global fit using the functional form:

$$e_v^q(x) = \kappa_q N_q x^{-\alpha_q} (1-x)^{\beta_q} (1 + \gamma_q \sqrt{x}), \quad (6)$$

where κ_q ($q = u, d$) are the quark magnetic moments, determined by the measured nucleon magnetic moments. It should also be noted that the normalization factor N_q is obtained from the following sum rule:

$$\int_0^1 dx e_v^q(x) = \kappa_q. \quad (7)$$

In high-energy processes involving nuclear targets, the partonic structure must be described by nPDFs rather than free proton PDFs to obtain accurate theoretical predictions. These nPDFs characterize the modified quark and gluon distributions within bound nucleons and are determined through global analyses of nuclear deep inelastic scattering and other hard processes [54–64] (see Ref. [65] for a recent review). These nuclear modifications extend to elastic scattering or hard exclusive processes involving nuclei, where nGPDs must replace the free nucleon GPDs. While the most rigorous approach to determine nGPDs at zero skewness is through a direct analysis of elastic electron-nucleus scattering data analogous to Refs. [30, 51] for the proton GPDs, current limitations in nuclear data availability motivate alternative strategies. Here, we explore the feasibility of constructing nGPDs by appropriately modifying free proton GPDs.

Following the classification in Appendix A of Ref. [61], we identify three distinct types of nPDFs:

1. **Bound nucleon nPDFs:** The distributions $f^{p/A}$ and $f^{n/A}$ describe bound protons and neutrons in a nucleus with mass number A , related through isospin symmetry ($u^{p/A} = d^{n/A}$, etc.).

2. **Average nucleon nPDF:** The nuclear-averaged distribution

$$f^{N/A}(x, \mu^2) = \frac{Z}{A} f^{p/A}(x, \mu^2) + \frac{A-Z}{A} f^{n/A}(x, \mu^2), \quad (8)$$

represents an isospin-weighted combination for a nucleus with charge Z .

3. **Nuclear nPDF:** The total nuclear distribution

$$f^A(x, \mu^2) = Z f^{p/A}(x, \mu^2) + (A-Z) f^{n/A}(x, \mu^2), \quad (9)$$

gives the complete parton content of the nucleus.

We correspondingly define three analogous types of nGPDs:

1. **Bound nucleon nGPDs:** Using the profile function $\mathcal{F}(x)$ from Eq. (5),

$$\begin{aligned} F^{p/A}(x, \mu^2, t) &= f^{p/A}(x, \mu^2) \exp[t\mathcal{F}^{p/A}(x)], \\ F^{n/A}(x, \mu^2, t) &= f^{n/A}(x, \mu^2) \exp[t\mathcal{F}^{n/A}(x)], \end{aligned} \quad (10)$$

with isospin symmetry assumed for both distributions and profile functions. Note that we have to assume that the profile functions are universal for different nuclei since we don't have their A -dependence at the present.

2. **Average nucleon nGPD:**

$$F^{N/A}(x, \mu^2, t) = \frac{Z}{A} F^{p/A}(x, \mu^2, t) + \frac{A-Z}{A} F^{n/A}(x, \mu^2, t). \quad (11)$$

3. **Nuclear nGPD:**

$$F^A(x, \mu^2, t) = Z F^{p/A}(x, \mu^2, t) + (A-Z) F^{n/A}(x, \mu^2, t). \quad (12)$$

Within this framework, one can employ the nPDFs from the nNNPDF Collaboration [66] at $\mu = 2$ GeV, maintaining consistency with the MMGPDs Collaboration's use of free-proton NNPDF PDFs [53] at the same scale for constructing proton GPDs. While this approach easily facilitates the construction of nuclear GPDs H , a significant challenge arises for GPDs E : currently, no nuclear modifications exist for their forward limits $e_v^q(x, \mu^2)$ from high-energy experimental data. To address this limitation in calculations requiring GPDs E , one can consider the following scenarios:

1. **No nuclear modification:** Proceed with calculations using only nuclear-modified valence PDFs $q_v(x, \mu^2)$, while keeping $e_v^q(x, \mu^2)$ unmodified from their free-nucleon forms.
2. **Universal nuclear modification:** Assume identical nuclear modification factors for $e_v^q(x, \mu^2)$ as those determined for the corresponding $q_v(x, \mu^2)$.

Nuclear transparency in GPDs language As discussed earlier, several studies have explored calculating nuclear transparency $T(Q^2)$ directly from GPDs [32, 33], typically defined as the ratio of nuclear to nucleon GPD integrals. While this approach provides valuable theoretical insight, we argue that a more robust determination of $T(Q^2)$ can be obtained by considering $T(Q^2)$ as the ratio of nuclear to nucleon differential cross-section $d\sigma/dQ^2$ or simply the reduced cross-section σ_R of the elastic electron-proton scattering. The reason is that the cross-section (whether differential or reduced) inherently incorporates contributions from both H and E GPDs, whereas the GPD-integral approach requires an ad hoc choice between these components (with Refs. [32, 33] selecting only H). Moreover, the cross-section is a quantity that is more relevant to the measured yields in Eq. (1) conceptually. This approach thus avoids the theoretical ambiguity in GPD selection while maintaining closer ties to experimental measurements.

According to the framework established in the previous section, we examine alternative approaches for calculating nuclear transparency $T(Q^2)$ using various nGPDs. We consider both GPD-based definitions and those tied directly to experimental observables like FFs and cross-sections. Following Ref. [32], we first investigate a GPD-based definition:

$$T(Q^2) = \frac{\left[\int_0^1 dx H^A(x, t) \right]^2}{\left[\int_0^1 dx H(x, t) \right]^2}, \quad (13)$$

where $H = H_v^u + H_v^d$ includes only valence quark contributions from GPD H (GPD E is ignored). Note that the cross-section of the (quasi)elastic electron-proton scattering is proportional to the electromagnetic FFs which are related only to the valence quark distributions.

For the numerator H^A , we employ the three nGPD variants, namely $F^{p/A}$, $F^{N/A}$, and F^A , using nNNPDF nPDFs [61] at $\mu = 2$ GeV. The denominator uses free proton GPDs from “Set11” of Ref. [67], based on NNPDF proton PDFs [53] at the same scale. Figure 1 shows our calculations of $T(Q^2)$ defined in Eq. (13) for Carbon nucleus using $H^{p/A}$ and $H^{N/A}$ nGPDs (labelled $T^{p/A}$ and $T^{N/A}$ respectively). We omit results using H^A nGPDs as they produce unphysically large $T(Q^2)$ values. The identical central values for both curves reflect Carbon’s isoscalar nature ($Z = A - Z$) or which the modifications of up quark distribution are the same as the ones of down quark distribution. As can be seen, the results obtained using Eq. (13) disagree with experimental measurements [34]. They even show decreasing $T(Q^2)$ with increasing Q^2 which contradicts QCD predictions for color transparency. It should be noted that the error bands shown in Fig. 1, as well as in all other figures throughout this paper, have been calculated using the standard Hessian method with $\Delta\chi^2 = 1$ [68], taking into account the uncertainties from both PDFs and GPDs.

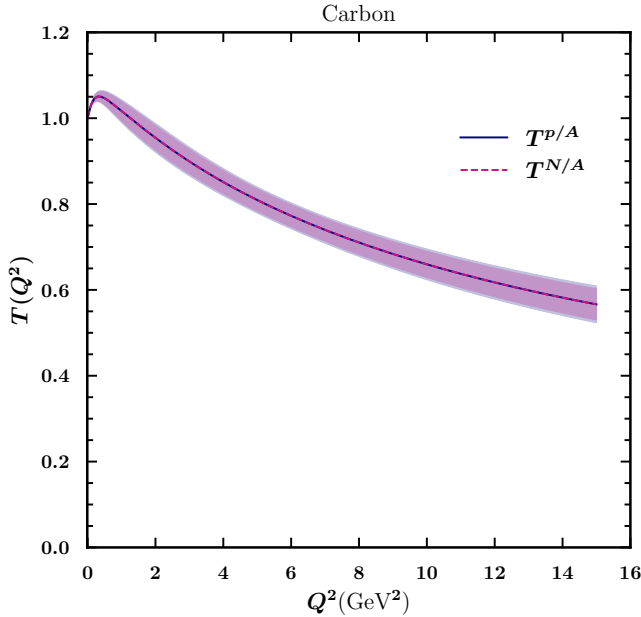


FIG. 1. A comparison between the results of $T(Q^2)$ for the Carbon nucleus obtained using $H^{p/A}$ and $H^{N/A}$ nGPDs, denoted as $T^{p/A}$ and $T^{N/A}$, respectively.

As previously discussed, we propose that the most accurate definition of nuclear transparency, $T(Q^2)$, can be obtained by replacing GPDs in Eq. (13) with the differential cross-section or reduced cross-section σ_R . However, before doing so, it is instructive to first connect $T(Q^2)$ to the Dirac form factor $F_1(Q^2)$, given its established relationship with the GPD H as shown in Eq. (2). This approach leads to the following

expressions for $T^{p/A}(Q^2)$ and $T^{N/A}(Q^2)$:

$$T^{p/A}(Q^2) = \frac{[F_1^{p/A}(Q^2)]^2}{[F_1^p(Q^2)]^2}, \quad T^{N/A}(Q^2) = \frac{[F_1^{N/A}(Q^2)]^2}{[F_1^p(Q^2)]^2}, \quad (14)$$

where the effective Dirac form factor for the nucleon in the nucleus, $F_1^{N/A}(Q^2)$, is given by:

$$F_1^{N/A}(Q^2) = e_u \int_0^1 dx (H_v^u)^{N/A}(x, t) + e_d \int_0^1 dx (H_v^d)^{N/A}(x, t), \quad (15)$$

with $(H_v^q)^{N/A}$ obtained from Eq. (11).

Just like before, the transparency $T^A(Q^2)$, when defined using the nuclear GPDs F^A from Eq. (12), yields unphysically large values. To address this, we suggest an alternative and more physically meaningful definition, inspired by the nuclear modification ratio R commonly used in the context of nuclear PDFs (see, e.g., Eq. (10) in Ref. [69]):

$$T^A(Q^2) = \frac{1}{A} \frac{[F_1^A(Q^2)]^2}{[F_1^p(Q^2)]^2}. \quad (16)$$

Figure 2 presents the resulting calculations for $T^{p/A}(Q^2)$, $T^{N/A}(Q^2)$, and $T^A(Q^2)$ based on the F_1 form factor in comparison with the experimental data of Refs. [34–38, 70] for Carbon nucleus. As shown, both $T^{p/A}(Q^2)$ and $T^{N/A}(Q^2)$ exhibit significant discrepancies with the experimental data [34], while the definition based on $T^A(Q^2)$ provides a much closer match to the observed trend.

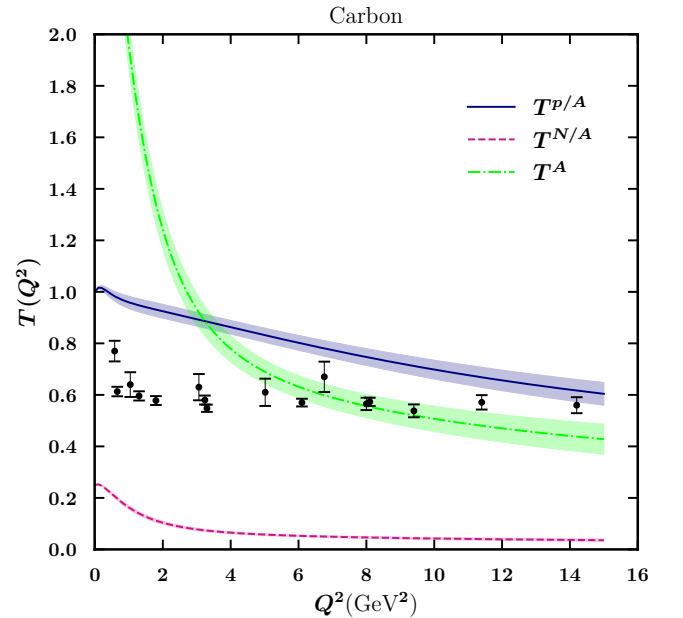


FIG. 2. Comparison of $T^{p/A}(Q^2)$, $T^{N/A}(Q^2)$, and $T^A(Q^2)$ derived from the Dirac form factor F_1 as defined in Eqs. (14) and (16) and the experimental data of Refs. [34–38, 70].

We now repeat the calculations by defining $T(Q^2)$ in terms of the ratio of reduced cross-sections, as follows:

$$T^{p/A}(Q^2) = \frac{\sigma_R^{p/A}(Q^2)}{\sigma_R^p(Q^2)}, \quad T^{n/A}(Q^2) = \frac{\sigma_R^{n/A}(Q^2)}{\sigma_R^n(Q^2)},$$

$$T^A(Q^2) = \frac{1}{A} \frac{\sigma_R^A(Q^2)}{\sigma_R^p(Q^2)}, \quad (17)$$

where σ_R expressed in terms of the Sachs electromagnetic FFs G_E and G_M as:

$$\sigma_R = \epsilon G_E^2(Q^2) + \tau G_M^2(Q^2). \quad (18)$$

These form factors are themselves related to the Dirac and Pauli form factors, F_1 and F_2 , as outlined in Eq. (3). The dimensionless kinematic variables ϵ and τ are given by:

$$\tau = \frac{Q^2}{4m^2}, \quad \epsilon = \left[1 + 2(1 + \tau) \tan^2\left(\frac{\theta}{2}\right) \right]^{-1}, \quad (19)$$

where m is the nucleon mass and θ is the electron scattering angle.

According to the equations above, if nuclear transparency $T(Q^2)$ is defined in terms of the reduced cross-section, then the contribution of the GPD E must also be taken into account, since the Pauli form factor F_2 is directly related to E . To carry out the calculations, we also require point-by-point values of the electron scattering angle θ in order to evaluate ϵ in Eq. (19). As θ is experiment-dependent, we simplify the calculation at this stage by assuming $\tan^2\left(\frac{\theta}{2}\right) = 1$.

Another important consideration is the nuclear modification of the GPD E . Unlike H , for which nuclear modifications can be constrained from high-energy data, corresponding modifications for E are not currently available as mentioned before. However, we can at least incorporate isospin effects by defining $(E_v^q)^{N/A}$ and $(E_v^q)^A$ as follows:

$$(E_v^q)^{N/A}(x, t) = \frac{Z}{A} (E_v^q)^{p/A}(x, t) + \frac{A-Z}{A} (E_v^q)^{n/A}(x, t),$$

$$(E_v^q)^A(x, t) = Z (E_v^q)^{p/A}(x, t) + (A-Z) (E_v^q)^{n/A}(x, t), \quad (20)$$

where $(E_v^q)^{p/A}$ and $(E_v^q)^{n/A}$ are taken to be the same as those for the free proton and neutron, respectively, in our calculations. Note that, according to our investigations, following scenario 2 mentioned before (Universal nuclear modification) does not lead to significant changes in the final results.

Figure 3 presents the results for $T^{p/A}(Q^2)$, $T^{n/A}(Q^2)$, and $T^A(Q^2)$, this time calculated using the reduced cross-section σ_R , in comparison with the experimental data of Refs. [34–38, 70]. As seen previously, both $T^{p/A}(Q^2)$ and $T^{n/A}(Q^2)$ show significant deviations from the experimental data. In contrast, the result for $T^A(Q^2)$ exhibits much better agreement with the data presented in Fig. 2 of Ref. [34].

It is important to note that the remaining discrepancy between our results for $T^A(Q^2)$ and the experimental data may arise from several sources:

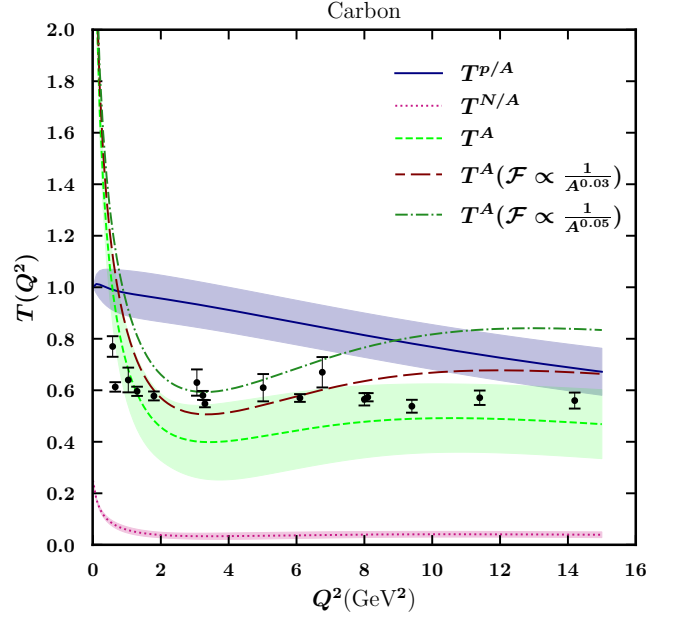


FIG. 3. Comparison of the results for $T^{p/A}(Q^2)$, $T^{n/A}(Q^2)$, and $T^A(Q^2)$, based on the reduced cross-section σ_R as defined in Eq. (17) and the experimental data of Refs. [34–38, 70].

- Nuclear modifications of the GPD E (more precisely e_v^q) have not been included, as such modifications are currently unavailable. Although we accounted for the isospin effect, it has no impact in the case of a carbon nucleus, which contains an equal number of protons and neutrons. However, it should be noted that assuming identical nuclear modification factors for e_v^q as those determined for the corresponding PDFs q_v (scenario 2) does not change the final results significantly.
- The profile functions \mathcal{F} have been treated as independent of the mass number A , which may be an oversimplification. If this assumption is incorrect, \mathcal{F} should exhibit A -dependence (more precisely, its individual parameters), and its functional form should ideally be determined through a global analysis of GPDs incorporating nuclear data. As an initial step, we introduce a simple A -dependent modification to \mathcal{F} in Eq. (5) and repeat the calculations to assess its impact on the results. Specifically, we consider $\mathcal{F} \propto \frac{1}{A^\alpha}$, inspired by analogous analyses in the context of nPDFs [71]. The corresponding results are shown as the long-dashed and dot-dashed curves in Fig. 3, for $\alpha = 0.03$ and $\alpha = 0.05$, respectively. As can be seen, this modification leads to an enhancement in the result, particularly at higher values of Q^2 . It should be noted that these values of α are chosen nominally to explore the magnitude of the change induced by considering an overall A -dependence in \mathcal{F} . Using negative values for α leads to a suppression of the final result. We emphasize that the true way to determine the A -dependence of \mathcal{F} is to make its parameters explicitly A -dependent and to extract their optimal

values through a fit to relevant data.

- For the results shown in Fig. 3 the scattering angle was assumed to be fixed ($\theta = 90^\circ$). To accurately reflect the experimental data, the calculations were repeated using the exact value of θ corresponding to each experimental data point. The updated results are displayed in Fig. 4, where the open circles represent the angle-corrected theoretical predictions. The change is negligible at high momentum transfer ($Q^2 \gtrsim 5 \text{ GeV}^2$), but it becomes significant at lower Q^2 . In the interval $3 < Q^2 < 4 \text{ GeV}^2$ the agreement with the data is modestly improved, whereas for $Q^2 < 2 \text{ GeV}^2$ the discrepancy grows. These observations confirm again the need to determine the exact A -dependence of the profile function \mathcal{F} through a dedicated fit to data. Note that individual parameters of \mathcal{F} may exhibit different A -dependencies since they govern distinct regions of Q^2 . The results, in particular, suggest a significant modification in the parameter α' , which governs the behavior at low Q^2 and may reflect the limits of this formalism at low energy scales.

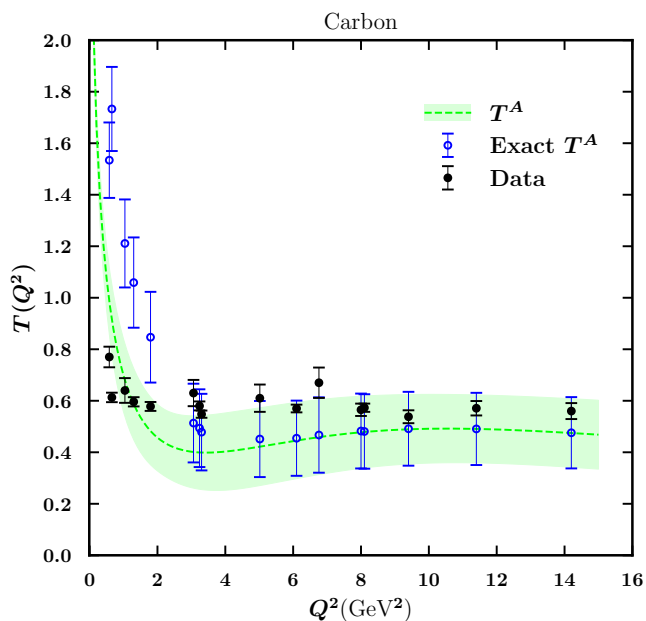


FIG. 4. Comparison of nuclear transparency calculations using an overall scattering angle $\theta = 90^\circ$ (dashed line) versus using the exact scattering angles corresponding to each data point (open circles). The experimental data are taken from Refs. [34–38, 70].

Conclusions In this work, we have revisited the phenomenon of nuclear transparency in the context of CT using the framework of GPDs. By constructing nGPDs from known nPDFs, we have introduced a consistent approach to describing exclusive scattering processes involving nuclei. Our study focused on the role of CT in high-energy exclusive processes, where the propagation of compact hadronic states through nuclear matter should, in principle, lead to a characteristic rise in transparency with increasing Q^2 . However, recent precision measurements of nuclear transparency in carbon nucleus [34] indicated an unexpected Q^2 -dependency that challenges this expectation.

To shed light on this issue, we calculated the nuclear transparency $T(Q^2)$ for the carbon nucleus considering various definitions and compared our theoretical predictions with available experimental data. Our results confirm that the choice of definition for $T(Q^2)$ remarkably affects the predicted behavior. Among the definitions considered, we find that the one most analogous to the nuclear modification ratio R commonly used at nuclear collisions [69] provides the best agreement with the observed nuclear transparency up to $Q^2 = 14.2 (\text{GeV}/c)^2$, as reported in recent measurements [34]. Additionally, we explored a simple A -dependent modification to the profile function \mathcal{F} used in the GPD parameterization. While this modification does impact the magnitude and trend of $T(Q^2)$, we emphasize that a more rigorous and reliable determination of nGPDs must be performed through a global analysis that incorporates nuclear data for different nuclei and kinematic conditions.

In conclusion, our findings highlight two key points: first, the definition of nuclear transparency should be carefully chosen to reflect the physical interpretation of medium modifications; second, achieving accurate and consistent results requires that the parameters of nGPDs be treated as nuclear-dependent and fitted through global analyses. These insights open new windows towards future studies aiming to improve our understanding of CT and the internal structure of hadrons in the nuclear environment.

Acknowledgements M. Goharipour thanks the Theoretical Physics Department at CERN for their kind hospitality during the period in which part of this work was carried out. F. Irani and K. Azizi are thankful to Iran National Science Foundation (INSF) for financial support provided for this research under grant No. 4033039.

[1] D. Dutta, K. Hafidi, and M. Strikman, *Prog. Part. Nucl. Phys.* **69**, 1 (2013), arXiv:1211.2826 [nucl-th].
[2] T. K. Choi, K.-J. Kong, and B.-G. Yu, *Phys. Rev. C* **111**, 064608 (2025), arXiv:2409.05129 [nucl-th].
[3] G. Barucca *et al.* (PANDA), *Eur. Phys. J. A* **57**, 184 (2021), arXiv:2101.11877 [hep-ex].

[4] F. Hauenstein *et al.*, *Phys. Rev. C* **105**, 034001 (2022), arXiv:2109.09509 [physics.ins-det].
[5] V. D. Burkert *et al.*, *Prog. Part. Nucl. Phys.* **131**, 104032 (2023), arXiv:2211.15746 [nucl-ex].
[6] O. Caplow-Munro and G. A. Miller, *Phys. Rev. C* **104**, L012201 (2021), arXiv:2104.11168 [nucl-th].

- [7] K. Gallmeister and U. Mosel, *MDPI Physics* **4**, 440 (2022), [arXiv:2202.12804 \[nucl-th\]](#).
- [8] S. J. Brodsky and G. F. de Teramond, *MDPI Physics* **4**, 633 (2022), [arXiv:2202.13283 \[hep-ph\]](#).
- [9] G. A. Miller, *MDPI Physics* **4**, 590 (2022), [arXiv:2203.02019 \[hep-ph\]](#).
- [10] G. M. Huber, W. B. Li, W. Cosyn, and B. Pire, *MDPI Physics* **4**, 451 (2022), [arXiv:2202.04470 \[hep-ph\]](#).
- [11] L. Frankfurt and M. Strikman, *MDPI Physics* **4**, 774 (2022), [arXiv:2210.11569 \[hep-ph\]](#).
- [12] S. Das, *Phys. Rev. C* **107**, 035201 (2023), [arXiv:2303.13214 \[nucl-th\]](#).
- [13] M. Diehl, *Phys. Rept.* **388**, 41 (2003), [arXiv:hep-ph/0307382](#).
- [14] X. Ji, *Ann. Rev. Nucl. Part. Sci.* **54**, 413 (2004).
- [15] A. V. Belitsky and A. V. Radyushkin, *Phys. Rept.* **418**, 1 (2005), [arXiv:hep-ph/0504030](#).
- [16] S. Boffi and B. Pasquini, *Riv. Nuovo Cim.* **30**, 387 (2007), [arXiv:0711.2625 \[hep-ph\]](#).
- [17] M. Diehl, *Eur. Phys. J. A* **52**, 149 (2016), [arXiv:1512.01328 \[hep-ph\]](#).
- [18] X.-D. Ji, *Phys. Rev. D* **55**, 7114 (1997), [arXiv:hep-ph/9609381](#).
- [19] X.-D. Ji, *J. Phys. G* **24**, 1181 (1998), [arXiv:hep-ph/9807358](#).
- [20] K. Goeke, M. V. Polyakov, and M. Vanderhaeghen, *Prog. Part. Nucl. Phys.* **47**, 401 (2001), [arXiv:hep-ph/0106012](#).
- [21] A. V. Belitsky, D. Mueller, and A. Kirchner, *Nucl. Phys. B* **629**, 323 (2002), [arXiv:hep-ph/0112108](#).
- [22] M. Guidal, H. Moutarde, and M. Vanderhaeghen, *Rept. Prog. Phys.* **76**, 066202 (2013), [arXiv:1303.6600 \[hep-ph\]](#).
- [23] K. Kumericki, S. Liuti, and H. Moutarde, *Eur. Phys. J. A* **52**, 157 (2016), [arXiv:1602.02763 \[hep-ph\]](#).
- [24] C. Mezrag, *Few Body Syst.* **63**, 62 (2022), [arXiv:2207.13584 \[hep-ph\]](#).
- [25] V. Bernard, L. Elouadrhiri, and U.-G. Meissner, *J. Phys. G* **28**, R1 (2002), [arXiv:hep-ph/0107088](#).
- [26] M. Guidal, M. V. Polyakov, A. V. Radyushkin, and M. Vanderhaeghen, *Phys. Rev. D* **72**, 054013 (2005), [arXiv:hep-ph/0410251](#).
- [27] M. Diehl and P. Kroll, *Eur. Phys. J. C* **73**, 2397 (2013), [arXiv:1302.4604 \[hep-ph\]](#).
- [28] M. V. Polyakov and P. Schweitzer, *Int. J. Mod. Phys. A* **33**, 1830025 (2018), [arXiv:1805.06596 \[hep-ph\]](#).
- [29] H. Hashamipour, M. Goharipour, and S. S. Gousheh, *Phys. Rev. D* **102**, 096014 (2020), [arXiv:2006.05760 \[hep-ph\]](#).
- [30] M. Goharipour, H. Hashamipour, F. Irani, and K. Azizi (MMGPDs), *Phys. Rev. D* **109**, 074042 (2024), [arXiv:2403.19384 \[hep-ph\]](#).
- [31] M. Goharipour, H. Hashamipour, H. Fatehi, F. Irani, K. Azizi, and S. V. Goloskokov (MMGPDs), (2025), [arXiv:2501.16257 \[hep-ph\]](#).
- [32] S. Liuti and S. K. Taneja, *Phys. Rev. D* **70**, 074019 (2004), [arXiv:hep-ph/0405014](#).
- [33] M. Burkardt and G. A. Miller, *Phys. Rev. D* **74**, 034015 (2006), [arXiv:hep-ph/0312190](#).
- [34] D. Bhetuwal *et al.* (Hall C), *Phys. Rev. Lett.* **126**, 082301 (2021), [arXiv:2011.00703 \[nucl-ex\]](#).
- [35] N. Makins *et al.*, *Phys. Rev. Lett.* **72**, 1986 (1994).
- [36] T. G. O'Neill *et al.*, *Phys. Lett. B* **351**, 87 (1995), [arXiv:hep-ph/9408260](#).
- [37] D. Abbott *et al.*, *Phys. Rev. Lett.* **80**, 5072 (1998).
- [38] K. Garrow *et al.*, *Phys. Rev. C* **66**, 044613 (2002), [arXiv:hep-ex/0109027](#).
- [39] A. S. Carroll *et al.*, *Phys. Rev. Lett.* **61**, 1698 (1988).
- [40] I. Mardor *et al.*, *Phys. Rev. Lett.* **81**, 5085 (1998).
- [41] A. Leksanov *et al.*, *Phys. Rev. Lett.* **87**, 212301 (2001), [arXiv:hep-ex/0104039](#).
- [42] J. Aclander *et al.*, *Phys. Rev. C* **70**, 015208 (2004), [arXiv:nucl-ex/0405025](#).
- [43] H. Meier-Hajduk, C. Hajduk, P. u. Sauer, and W. Theis, *Nucl. Phys. A* **395**, 332 (1983).
- [44] L. Frankfurt, G. A. Miller, and M. Strikman, *Phys. Lett. B* **304**, 1 (1993), [arXiv:hep-ph/9305228](#).
- [45] L. L. Frankfurt and M. I. Strikman, *Phys. Rept.* **160**, 235 (1988).
- [46] L. Frankfurt, M. Strikman, and C. Weiss, *Ann. Rev. Nucl. Part. Sci.* **55**, 403 (2005), [arXiv:hep-ph/0507286](#).
- [47] W. A. Horowitz and M. Gyulassy, *Nucl. Phys. A* **872**, 265 (2011), [arXiv:1104.4958 \[hep-ph\]](#).
- [48] T. Lappi and H. Mantysaari, *Phys. Rev. C* **87**, 032201 (2013), [arXiv:1301.4095 \[hep-ph\]](#).
- [49] M. Kordell and A. Majumder, *Phys. Rev. C* **97**, 054904 (2018), [arXiv:1601.02595 \[nucl-th\]](#).
- [50] A. B. Larionov, *Phys. Part. Nucl.* **56**, 381 (2025).
- [51] M. Goharipour, F. Irani, H. Hashamipour, and K. Azizi (MMGPDs), *Phys. Lett. B* **864**, 139423 (2025), [arXiv:2408.01783 \[hep-ph\]](#).
- [52] M. Diehl, T. Feldmann, R. Jakob, and P. Kroll, *Eur. Phys. J. C* **39**, 1 (2005), [arXiv:hep-ph/0408173](#).
- [53] R. D. Ball *et al.* (NNPDF), *Eur. Phys. J. C* **82**, 428 (2022), [arXiv:2109.02653 \[hep-ph\]](#).
- [54] D. de Florian, R. Sassot, P. Zurita, and M. Stratmann, *Phys. Rev. D* **85**, 074028 (2012), [arXiv:1112.6324 \[hep-ph\]](#).
- [55] K. Kovarik *et al.*, *Phys. Rev. D* **93**, 085037 (2016), [arXiv:1509.00792 \[hep-ph\]](#).
- [56] K. J. Eskola, P. Paakkinen, H. Paukkunen, and C. A. Salgado, *Eur. Phys. J. C* **77**, 163 (2017), [arXiv:1612.05741 \[hep-ph\]](#).
- [57] R. Wang, X. Chen, and Q. Fu, *Nucl. Phys. B* **920**, 1 (2017), [arXiv:1611.03670 \[hep-ph\]](#).
- [58] H. Khanpour, M. Soleymaninia, S. Atashbar Tehrani, H. Spiesberger, and V. Guzey, *Phys. Rev. D* **104**, 034010 (2021), [arXiv:2010.00555 \[hep-ph\]](#).
- [59] K. J. Eskola, P. Paakkinen, H. Paukkunen, and C. A. Salgado, *Eur. Phys. J. C* **82**, 413 (2022), [arXiv:2112.12462 \[hep-ph\]](#).
- [60] P. Duventäster, T. Ježo, M. Klasen, K. Kovařík, A. Kusina, K. F. Muzakka, F. I. Olness, R. Ruiz, I. Schienbein, and J. Y. Yu, *Phys. Rev. D* **105**, 114043 (2022), [arXiv:2204.09982 \[hep-ph\]](#).
- [61] R. Abdul Khalek, R. Gauld, T. Giani, E. R. Nocera, T. R. Rabemananjara, and J. Rojo, *Eur. Phys. J. C* **82**, 507 (2022), [arXiv:2201.12363 \[hep-ph\]](#).
- [62] I. Helenius, M. Walt, and W. Vogelsang, *Phys. Rev. D* **105**, 094031 (2022), [arXiv:2112.11904 \[hep-ph\]](#).
- [63] C. Flore, C. Hadjidakis, D. Kikola, A. Kusina, and A. Safronov, *Phys. Lett. B* **866**, 139554 (2025), [arXiv:2503.21531 \[hep-ph\]](#).
- [64] M.-Q. Yang, P. Ru, and B.-W. Zhang, (2025), [arXiv:2505.04906 \[hep-ph\]](#).
- [65] M. Klasen and H. Paukkunen, *Ann. Rev. Nucl. Part. Sci.* **74**, 49 (2024), [arXiv:2311.00450 \[hep-ph\]](#).
- [66] R. Abdul Khalek, J. J. Ethier, J. Rojo, and G. van Weelden, *JHEP* **09**, 183 (2020), [arXiv:2006.14629 \[hep-ph\]](#).
- [67] H. Hashamipour, M. Goharipour, K. Azizi, and S. V. Goloskokov, *Phys. Rev. D* **107**, 096005 (2023), [arXiv:2211.09522 \[hep-ph\]](#).
- [68] J. Pumplin, D. Stump, R. Brock, D. Casey, J. Huston, J. Kalk, H. L. Lai, and W. K. Tung, *Phys. Rev. D* **65**, 014013 (2001), [arXiv:hep-ph/0101032](#).
- [69] M. Goharipour and H. Mehraban, *Phys. Rev. D* **95**, 054002 (2017), [arXiv:1702.05738 \[hep-ph\]](#).
- [70] G. Garino *et al.*, *Phys. Rev. C* **45**, 780 (1992).
- [71] M. Hirai, S. Kumano, and T. H. Nagai, *Phys. Rev. C* **76**, 065207

(2007), arXiv:0709.3038 [hep-ph].